water

MDPI

Article

Evaluating Land Subsidence Rates and Their Implications for Land Loss in the Lower Mississippi River Basin

Lei Zou [1,*], Joshua Kent [2], Nina S.-N. Lam [1], Heng Cai [1], Yi Qiang [1] and Kenan Li [1]

Received: 5 November 2015; Accepted: 17 December 2015; Published: 26 December 2015
Academic Editor: Richard Smardon

[1] Department of Environmental Sciences, Louisiana State University, 1285 Energy, Coast & Environment Building, Louisiana State University, Baton Rouge, LA 70803, USA; nlam@lsu.edu (N.S.-N.L.); hcai1@lsu.edu (H.C.); yqiang1@lsu.edu (Y.Q.); kli4@lsu.edu (K.L.)
[2] Center for GeoInformatics, Louisiana State University, 200 Engineering Research & Development Building, Louisiana State University, Baton Rouge, LA 70803, USA; jkent4@lsu.edu
* Correspondence: lzou4@lsu.edu; Tel.: +1-573-256-9706; Fax: +1-225-578-4286

Abstract: High subsidence rates, along with eustatic sea-level change, sediment accumulation and shoreline erosion have led to widespread land loss and the deterioration of ecosystem health around the Lower Mississippi River Basin (LMRB). A proper evaluation of the spatial pattern of subsidence rates in the LMRB is the key to understanding the mechanisms of the submergence, estimating its potential impacts on land loss and the long-term sustainability of the region. Based on the subsidence rate data derived from benchmark surveys from 1922 to 1995, this paper constructed a subsidence rate surface for the region through the empirical Bayesian kriging (EBK) interpolation method. The results show that the subsidence rates in the region ranged from 1.7 to 29 mm/year, with an average rate of 9.4 mm/year. Subsidence rates increased from north to south as the outcome of both regional geophysical conditions and anthropogenic activities. Four areas of high subsidence rates were found, and they are located in Orleans, Jefferson, Terrebonne and Plaquemines parishes. A projection of future landscape loss using the interpolated subsidence rates reveals that areas below zero elevation in the LMRB will increase from 3.86% in 2004 to 19.79% in 2030 and 30.88% in 2050. This translates to a growing increase of areas that are vulnerable to land loss from 44.3 km^2/year to 240.7 km^2/year from 2011 to 2050. Under the same scenario, Lafourche, Plaquemines and Terrebonne parishes will experience serious loss of wetlands, whereas Orleans and Jefferson parishes will lose significant developed land, and Lafourche parish will endure severe loss of agriculture land.

Keywords: subsidence rates; Mississippi Delta; coastal Louisiana; land loss; sustainability; Bayesian kriging

1. Introduction

The Lower Mississippi River Basin (LMRB) located in southeastern coastal Louisiana is a major producer of crude oil and natural gas in the U.S., containing a large portion (40%–45%) of the nation's coastal wetlands and acting as a buffer zone for in-land residents from hurricanes and storms [1]. Since 1930, however, this area has lost more than 4921 km^2 (~1900 mi^2) of land, which accounts for 80% of the total coastal wetland loss in the U.S. [2]. The land loss problem causes severe damage to local fishery industries, deteriorates wetland ecosystem balance and increases the risk of coastal hazards to both coastal residents and energy infrastructures, which may cause thousands of fatalities and billions of economic loss. The widespread land loss around coastal Louisiana stemmed from the combination of land subsidence, eustatic sea-level change and shoreline erosion [3]. However, high subsidence rates

have been considered a principal cause contributing to the ongoing extensive wetland loss in coastal Louisiana [4].

Subsidence is defined as the downward shifting of land surface relative to a reference datum. Due to its impacts on the economy, livelihood and culture, a number of researchers have attempted to evaluate the subsidence rates in coastal Louisiana using different approaches, including analyses based on discrete tide gauge records [5] or benchmarks surveys [6], numerical modeling [7] and RADARSAT satellite images [8]. Similarly, different factors driving the subsidence process have been investigated quantitatively, including consolidation of Holocene sediments, sediment loadings, sea-level rise, movements on growth faults and hydrocarbon production [9].

Despite these prior studies, few investigations examining vertical change in coastal Louisiana have focused on creating an accurate subsidence rate surface to reveal the spatial patterns and potential impacts on the region's long-term sustainability. The objectives of this investigation are three-fold. First, we will create a subsidence rate surface in the study area using the empirical Bayesian kriging (EBK) interpolation method. Second, future elevation will be projected based on the calculated subsidence rates. Third, possible land loss impacts caused by subsidence induced elevation change will be estimated. This study is significant in that it provides scenarios of future environmental changes caused by land subsidence in the deltaic region. The knowledge gained can be used to support decision makers to formulate plans for mitigation, adaptation and restoration in advance.

The remainder of this paper is organized as follows. Section 2 describes the study area and previous related studies. Section 3 introduces the major data sources and methods to create the subsidence rate layer. Section 4 presents the results, and the land loss implications are discussed on Section 5. Section 6 presents the conclusions of this study.

2. Study Area

The Lower Mississippi River Basin (LMRB) is located in southeastern Louisiana, the United States (Figure 1), with elevation ranging from −7.3 to 370 meters and a mean of 10.7 meters. The study region consists of 26 parishes, covering the cities of New Orleans and Baton Rouge, 63 watersheds and three basins—Lake Pontchartrain, Terrebonne and Barataria basins [10]. Its total area is around 48,046 km^2. The Mississippi River flows into the LMRB from West Feliciana Parish in the northwest to the Plaquemines Parish in the southeast and eventually discharges to the Gulf of Mexico.

The study region is extremely vulnerable to land subsidence, which is the result of complex interactions among natural, social and economic conditions. Frequently exposed to hurricanes and storms, southern Louisiana is particularly vulnerable to coastal inundation hazards. A study on business recovery in New Orleans after Hurricane Katrina confirmed that flood depth is significantly negatively correlated with business reopening probabilities [11]. It is projected that Katrina-like storm surges will hit every other year if the climate warms 2 °C (~3.6 °F) [12]. Ongoing sinking will exacerbate these hazards and further delay recovery processes. The consequences of subsidence extend beyond flooding. Research has closely linked subsidence with land loss observed across the coastal zone. Reed and Cahoon (1993) suggested that a slight downwards shifting in elevation can lead to frequent flooding, which would erode vegetation and further accelerate the loss of wetlands in these areas [13]. Aerial monitoring showed that the statewide wetland loss rates in Louisiana were 36 km^2/year, 100 km^2/year and 65 km^2/year during 1930–1950, 1960–1980 and 1980–1990, respectively [14]. Unchecked erosion brings the Gulf of Mexico closer to human habitats, raising the public's concerns about the future sustainability of subsiding communities. Wetland losses also threaten energy infrastructure. As a major supplier of crude oil with many gas wells and pipelines beneath the low elevation area, the relative sea level rise associated with subsidence and global eustasy will expose facilities to seawater, which can immerse coastal soils, corrode the energy facilities, as well as increase the risk of damage to energy infrastructures.

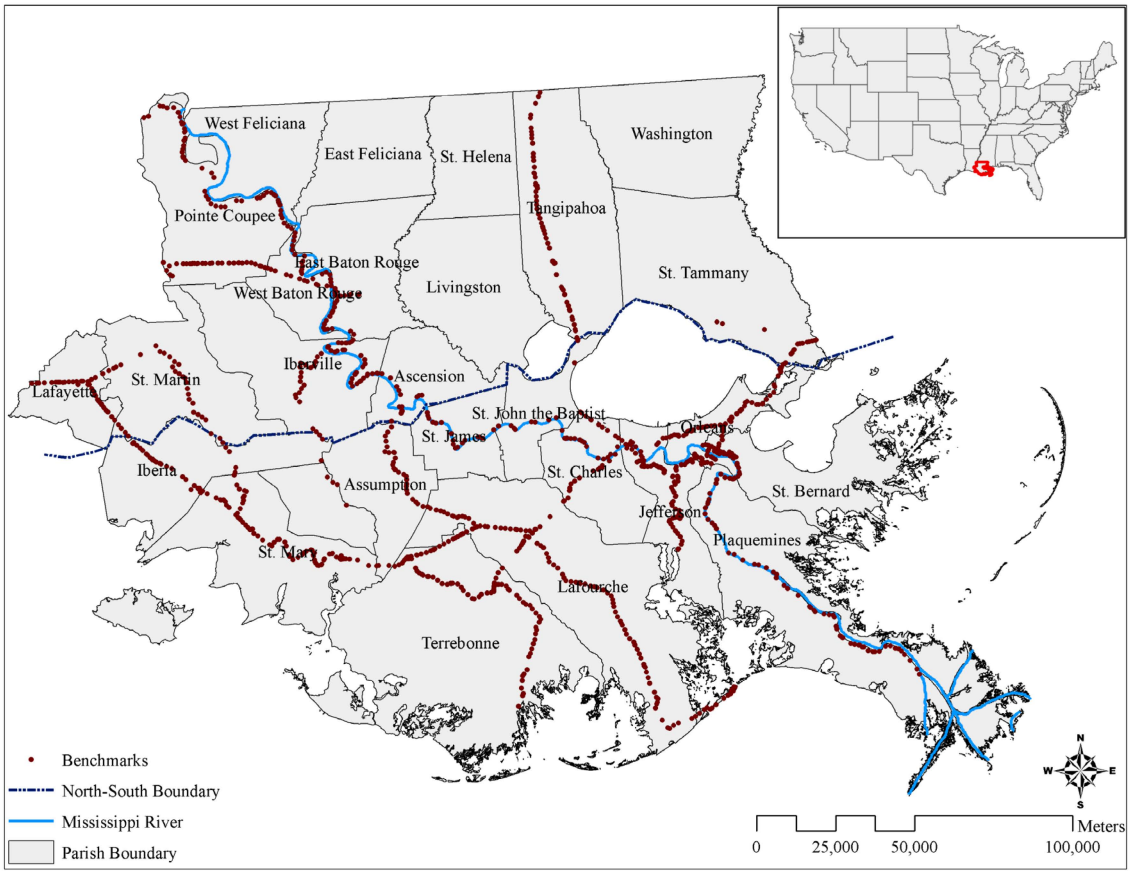

Figure 1. The Lower Mississippi River Basin (LMRB).

Several studies have attempted to estimate subsidence rates in coastal Louisiana. Based on the stationary drilling data, Roberts *et al.* (1994) found that the average subsidence rates increased an order of magnitude (0.43–3.96 mm/year) from west to east and doubled (2.17–4.29 mm/year) from north to south around the Mississippi River Delta [15]. Surveys by Penland and others [5,16–18] concluded that subsidence rates for the Mississippi Deltaic plain were 9–13 mm/year. Using the 2710 benchmarks during 1920 and 1995, Shinkle and Dokka (2004) found that the subsidence rates were substantially higher than rates reported in previous studies with a maximum rate of 51.92 mm/year, and the rates increased in many areas during the latter half of the 20th century [6]. Further, Kent and Dokka (2013) utilized ordinary kriging spatial interpolation to estimate subsidence rates in coastal Louisiana, resulting in rates with a range of 3–17 mm/year [19].

To thoroughly capture the mechanism of downward shifting phenomenon in the LMRB, factors from environmental process and human activities should be considered and quantitatively measured. Four factors have been frequently mentioned in the literature, including geological factors, such as consolidation of Holocene sediments, lithospheric flexure response to sediment loadings, tectonic movements on growth faults and anthropogenic factors, mostly human-induced fluid extraction and hydrocarbon production [20–24]. Yuill *et al.* (2009) found that the range of rates caused by the four factors were 1.0–8.0, 1.0–5.0, 0.1–20 and 0–3 mm/year [9]. Chan (2007) and Mallman and Zoback (2007) concluded that the combination of the first three environmental processes explained only about a 3-mm/year subsidence rate, whereas vertical change caused by hydrocarbon production induced fault reactivation, and reservoir compaction was primary responsible for the high subsidence rates, as the change of hydrocarbon production volumes coincide with the changes of land loss rates during 1920 and 1995 [1,25].

These previous studies on subsidence rates in this region were mostly based on an analysis of discrete points. However, the influence of land submergence is statewide and area based. An accurate evaluation of the spatial pattern and trend of subsidence rates can give new insights into the land loss problem. This study aims to build a bridge between current field measurements and regional influences of subsidence by interpolating the sampled point values into a continuous surface and to comprehend its impacts at a broader scale. Since the coastal zone is adjacent to open water and has suffered significant land loss during the past decade, the study area is divided into the north and the south regions according to the boundary along the northern shoreline of Lake Pontchartrain (Figure 1), to compare the subsidence rates and their potential impacts caused by subsidence between inland and coastal zones [26]. This imaginary boundary roughly divides areas that have experienced significant population growth (the north) and areas that have suffered long-term population decline (the south).

3. Data and Methods

3.1. Data Sources

Technical Report #50 (TR50) provides the most comprehensive geodetic study of vertical change ever conducted for the Louisiana Gulf coast [6]. The report, published by the National Geodetic Survey (NGS), assessed vertical change for 2710 discrete reference benchmarks observed during 96 first-order geodetic leveling surveys conducted between 1920 and 1995. Relative differences in height were measured for observations that coincided with two or more surveys. To account for decades of uncorrected subsidence, benchmark heights were validated by using vertical change estimates derived from relative sea-level rates measured at tide gauges associated with the leveling surveys [6]. Because the heights measured at each benchmark were minimally constrained (*i.e.*, tied only to one known benchmark), the relative displacements between survey epochs were free from errors and distortions that typically propagate within constrained network adjustments [6]. The subsidence rate for each benchmark location was determined by the difference between the two most recent measurements divided by the number of gap years and then subtracting the global sea-level rise rate:

$$R_{subsidence} = \frac{H_{end} - H_{begin}}{Y_{end} - Y_{begin}} - R_{sea-level-rise} \quad (1)$$

In Equation (1), $R_{subsidence}$ and $R_{sea-level-rise}$ represent the yearly subsidence and sea-level-rise rates, respectively. Y_{begin} and Y_{end} stand for the beginning and ending years of the survey period, and H_{begin} and H_{end} are the corresponding elevation readings of the benchmark at the beginning and the ending years. Shinkle and Dokka adopted a constant sea-level rise rate of 1.25 mm/year. Of the 1178 benchmarks located in the LMRB (Figure 1), 385 sites are located in the north, and their rates ranged from −0.42 mm/year (meaning no subsidence, but rather, minor uplifting) to 49.28 mm/year, with an average rate of 7.72 mm/year. The other 777 locations are in the south, and their subsidence rates ranged from 0.0 to 51.94 mm/year with a mean of 10.95 mm/year.

Other data involved in this study include elevation and land use/land cover products. Elevation data were obtained from the National Elevation Dataset (NED) of the U.S. Geological Survey (USGS), updated in 2004. Land use and land cover data were acquired from the National Land Cover Database (NLCD). Before analysis, the original 15 land cover types were re-aggregated to the 7 categories corresponding to Anderson's first-level LULC classification [27], and they include water, developed land, barren, forest, grass, agricultural land and wetlands. The resolutions for both datasets were 30 × 30 meters.

3.2. Empirical Bayesian Kriging

To create a subsidence rate surface accurately in the study area based on the sample points, it is necessary to choose a suitable spatial interpolation method to estimate values at unknown locations from observed values. Kriging is a popular geo-statistical interpolation technique that returns the

best linear unbiased prediction of the intermediate data and avoids cluster effects, which is especially important for this investigation, since our data are quite spatially clustered. Kriging assumes that the spatial variation of an attribute consists of a trend *m(Z)* and a spatially-correlated component [28]:

$$Z_0 = m(Z) + \sum_{i=1}^{m} W_i \times (Z_i - m(Z_i)) \quad (2)$$

where Z_0 is the estimated value at one unknown location, m is the number of points in a neighborhood and W_i and Z_i are the weights and observed values of the i-th surrounding observation, respectively. Different treatments of the three components—the trend, the residual variogram and the error term—led to the development of various kriging methods [29]. Here, we will briefly explain the principle of ordinary kriging assumed without a trend component as an example. To measure the spatially-correlated component, ordinary kriging uses isotropic semivariance, which is computed as:

$$\gamma(h) = \frac{1}{2} \times E\left[(Z(0) - Z(h))^2\right] \quad (3)$$

where $\gamma(h)$ is computed as half of the average squared difference between one location and another at a distance of h, with their values *Z(0)* and *Z(h)*. The relationship between lag distance and corresponding semivariance is described as a model, such as spherical, exponential and Gaussian, with parameters nugget, sill and range [30]. The weights of the surrounding observations are determined through the semivariance matrix between data points:

$$\begin{bmatrix} W \\ \lambda \end{bmatrix} = \begin{bmatrix} V & 1 \\ 1 & 0 \end{bmatrix}^{-1} \times \begin{bmatrix} D \\ 1 \end{bmatrix} \quad (4)$$

where W is the vector of weights, V is the semivariance matrix between surrounding known data pairs and D is the semivariance between unknown and known points. Lagrange multiplier λ is added to guarantee the minimum estimation error subject to the constraint that the sum of weights is equal to 1. An advantage of this interpolation routine is that the standard error for each estimate can be calculated and mapped according to:

$$\sigma^2 = \sum_{i=1}^{n} W_i \times \gamma(h_{i0}) + \lambda \quad (5)$$

where σ is the standard error and $\gamma(h_{i0})$ is the semivariance between the i-th known points and the point to be estimated. A kriging error map can be used to indicate where future sampling should be conducted to reduce the interpolation error [31]. However, classical kriging assumes that data are generated from a Gaussian distribution with the correlation structure defined by the estimated semivariogram, which is difficult to establish in practice.

Bayesian statistics provides a statistically-robust approach for modeling the uncertainties with respect to the unknown distribution and parameters of the input samples [32]. Empirical Bayesian kriging (EBK) combines Bayes' theorem and kriging interpolation and accounts for the error in estimating the true semivariogram through iterative simulations [33]. Figure 2 explains the procedures of EBK interpolation used in this investigation. First, the input sample data are divided into I subsets with less than or equal to N samples. For each subset, observations are transformed to a Gaussian distribution, and a semivariogram model is derived. Based on the semivariogram, new data are simulated and back transformed at known points. This process is iterated for n times, and each time, the new data produces a new semivariogram. Using Bayes' rule, the weights for each semivariogram are computed:

$$W(\theta_i \mid Z) = f(Z \mid \theta_i) \times P(\theta_i) \quad (6)$$

where θ_i is the i-th set of semivariogram parameters nugget, sill and range. $W(\theta_i \mid Z)$ is the weight for the i-th semivariogram; $f(Z \mid \theta_i)$ evaluates the likelihood the observed data can be generated from the semivariogram; and $P(\theta_i)$ stands for the probability of the i-th set of parameters θ_i among the simulated semivariogram spectrum. The weighted sum of simulated semivariograms creates a "true" semivariogram model. For each location, the prediction is generated using the "new" semivariogram distribution in the point's neighborhood. Compared to classical kriging, EBK is more appropriate for interpolating non-stationary data for large areas and requires less sample data [32].

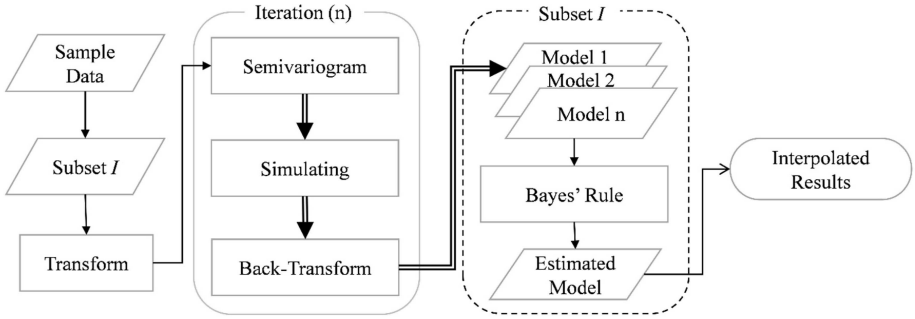

Figure 2. Procedures of empirical Bayesian kriging (EBK).

4. Results

In this investigation, the number N of data points in each subset was set to 100. For each subset of data, an empirical transformation was applied to satisfy the assumption of normality. The overlap factor x representing the number of subsets in which an observation will participate was set to 1.0 (meaning each observation is only being considered once), and the number of simulated semivariograms n was 100. The neighborhood search radius R was defined as 86 kilometers, which was determined by Moran's I autocorrelation analysis as the distance at which Moran's I is the highest [34]. Since the output pixel size is 30 × 30 meters, which is very time consuming for a study area with nearly 50 million pixels, we used the parallel computing option available in ArcGIS to accelerate the processing. The parameter was set to 100%, meaning that all of the cores in a computer were used in parallel computing. It took 490 h to complete the whole process on an eight-core CPU workstation.

Figure 3 and Table 1 shows the interpolated subsidence rates. There are active areas with high subsidence rates above 20 mm/year. They are located at Terrytown in Jefferson parish (#1), southern Orleans parish along the Intracoastal Waterway (#2), the wetlands between Morgan City and Houma in Terrebonne parish (#3) and the deltaic zones around the Triumph community in Plaquemines parish (#4). The standard errors of the estimated interpolated rates were less than 2.5 mm/year in 53.12% and less than 5 mm/year in 91.84% of the research area (Figure 4). Higher estimation errors are generally located in the southeastern part of coastal Louisiana and selected areas in New Orleans.

We compared our estimation to previous investigations at the same location for further evaluation (Table 2). We also conducted an interpolation using ordinary kriging (OK) for comparison. All subsidence rates in the table are expressed as millimeters per year. In the New Orleans metropolitan area, interpolated rates from EBK are similar to the observations from Dixon *et al.* (2006) [8] and Louisiana's coastal master plan [35], whereas the EBK interpolated values at southern Lafourche and Terrebonne parishes are slightly higher than the previous surveys by Boesch *et al.* (1983), Roberts *et al.* (1994) and Mallman and Zoback (2007) [15,25,36]. In the Mississippi River Delta around Plaquemines parish, previous studies [34,35] derived a faster subsidence rate than EBK calculation. In addition to the studies listed in Table 2, several investigations, including Burkett *et al.* (2003), Morton *et al.* (2002), Morton *et al.* (2005), Ivins *et al.* (2007) and Kent *et al.* (2013) [25,37–39], have used the same TR50 benchmark survey data from NGS and obtained similar subsidence estimations at various parts of the study region. Consistency between ranges in different sets of results demonstrated that our

interpolation is reliable and accurate. Furthermore, a comparison between EBK and OK shows that interpolated subsidence rates from EBK are closer to previous studies than the values derived by OK.

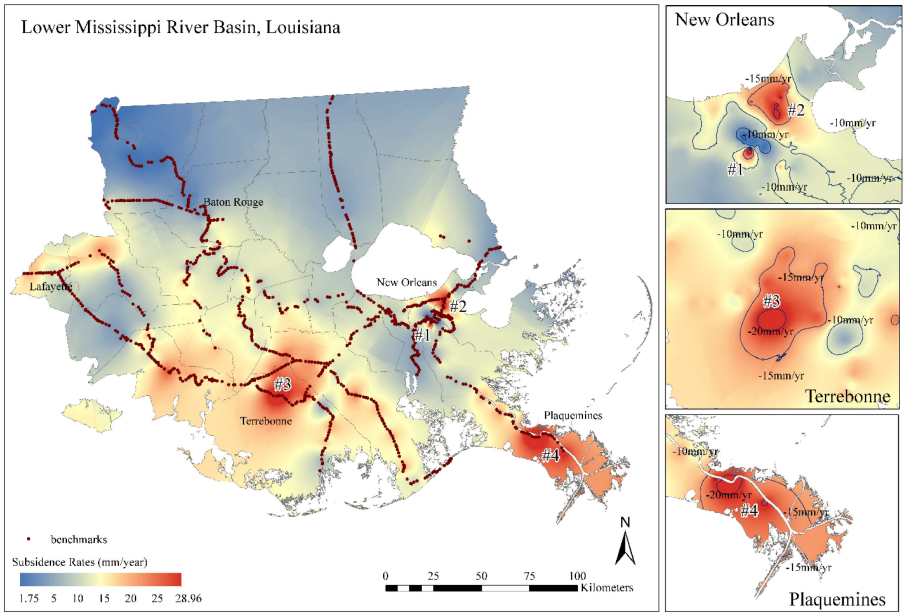

Figure 3. Interpolated subsidence-rate map in the Lower Mississippi River Basin.

Table 1. Statistics of interpolated subsidence rates.

Statistical Area	Min (mm/year)	Max (mm/year)	Average (mm/year)
The North	1.93	16	7.55
The South	1.75	28.96	11.02
The LMRB	1.75	28.96	9.25

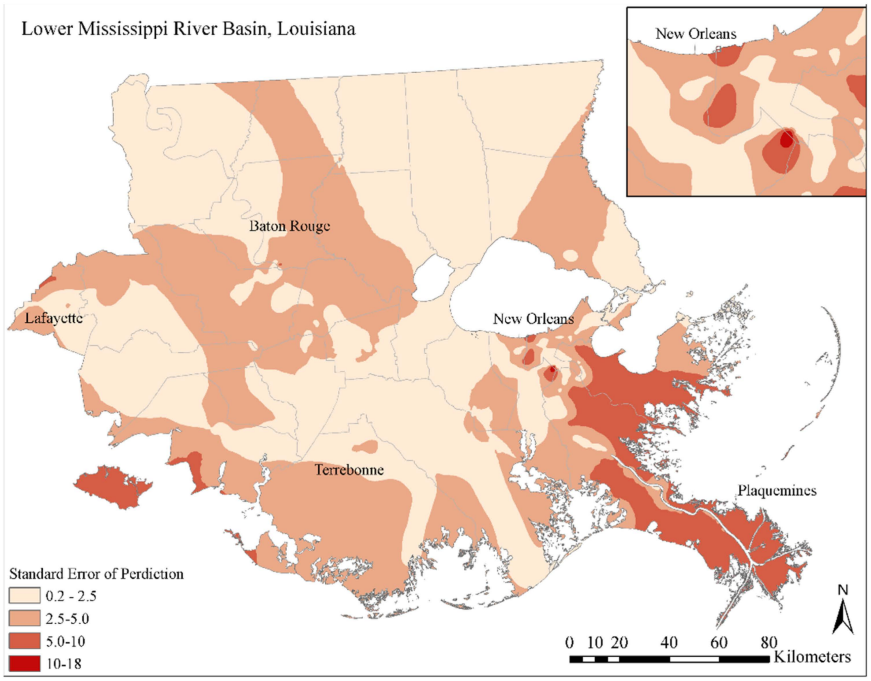

Figure 4. Standard errors of interpolated subsidence rates.

Table 2. Subsidence rates (in mm/year) from the literature and our results.

Author	Method	Period	Study Region	Rates	Ordinary Kriging	Empirical Bayesian Kriging (Our Results)
Boesch *et al.*, 1983 [15]	Tide gauge	1970–1980	Wetlands along Gulf of Mexico	mean = 10	8.04–17.19, mean = 12	5.76–14.38, mean = 11.2
			Mississippi River Delta	max = 40	11.11–22.48, max = 22.48	12.4–24, max = 24
Roberts *et al.*, 1994 [25]	Drill	1990–1993	Southern Terrebonne and St. Mary	0.43–4.29	8.73–16.58	7.72–12
Dixon, *et al.*, 2006 [8]	RADARSAT monitoring	2002–2005	New Orleans City	10.3–28.6, mean = 8	3.03–20.35, mean = 10.9	1.75–28.96, mean = 10.7
Lane *et al.*, 2006 [40]	Elevation monitoring stations	1996–2000	Caernarvon wetlands	5.9–12.1	8.32–11.65	9.52–10.45
			West Point A La Hache wetlands	5.4–12.7	10.56–13.60	9.66–14.31
			Violet wetlands	15.4–27.8	11.08–15.60	10.2–16.57
Mallman & Zoback, 2007 [36]	Numerical modeling	1982–1993	Southern Lafourche	5–10	7.48–15.52	5.76–16.7
Peyronnin *et al.*, 2013 [35]	Literature and experts panel	Current and near future	Mississippi River Delta	15–35	11.11–22.48	12.4–24
			Wetlands along Gulf of Mexico	6–20	8.04–17.19	5.76–14.38
			New Orleans City	2–35	3.03–20.35	1.75–28.96

In general, subsidence rates are lower in the north inland area and higher in the south coastal zone (Figure 3 and Table 1). This north-south discrepancy is hypothesized as the outcome of both regional geophysical conditions and anthropogenic activities. The south zone contains numerous submerged vertical faults. For instance, Thibodaux fault crosses the city of New Orleans, and Theriot and Golden Meadow faults pass through St. Mary, Terrebonne, Lafourche and Plaquemines parishes [41,42]. The structure of the Mississippi Delta is largely based on deposited salt structures derived from an underlying autochthonous Jurassic salt [43]. The upward intrusion of salt into fault zones, known as "salt diapir", may trigger proximally located faults and create new radial fault zones, thus contributing to land sinking. Another significant factor is sediment compaction, which is strongly affected by human activities. Hydrocarbon production has had a significant presence in the South for more than a century. Withdrawal of subsurface petroleum, natural gas and significant quantities of groundwater triggers the loss of subsurface pore pressure, which in turn accelerates natural consolidation processes and increases the degree of land subsidence [7,21]. Theoretically, both the tectonic and anthropogenic processes are localized, with the former being a longer term process. Previous investigations in coastal Louisiana suggested that long-term fault slip led to a 0.1–20 mm/year subsidence rate, and human activities aggravated the subsidence process by contributing up to a 23 mm/year subsidence rate in some areas [9,23,44].

All four high subsidence areas are located in the south zone, including two locations in greater New Orleans. The urban growth of New Orleans has led to extensive networks of pumps and canals designed to move water away from residential areas. These canals and pumps were mostly positioned on the natural levee of the Mississippi River. As the city grew, the pumps and canals were expanded to move water into Lake Pontchartrain. Seasonal high water levels and the threat from storm surge triggered levee construction along the river and related industrial navigation canals, disconnecting the soils from the natural hydrography and triggering sediment compaction and consolidation. Meanwhile, the wet and dry process caused by precipitation and pumping activities extracts water from the ground, making soil particles collapse onto each other and inducing more subsidence. Furthermore, tapping into subsurface aquifers for industrial purposes could activate fault slip and shallow surface deformations, particularly in New Orleans East [45].

Another two hotspots are located in the coastal wetlands in Terrebonne and Plaquemines parishes. The Terrebonne Basin located in Terrebonne parish consists of thick uncompacted sediment areas and is subject to high compaction, which contributes to high subsidence [46]. Although human-related hydrocarbon production could induce surficial changes and subsidence, whether this factor has contributed to high subsidence in the Terrebonne Basin remains controversial. Coleman and Roberts (1989) and Boesch *et al.* (1994) [3,47] concluded that the production impacts on wetland subsidence are minimal, while Morton *et al.* (2003) [48] speculated that the high density of oil/gas wells and related energy infrastructures may be associated with higher levels of land subsidence. On the other hand, human activities were considered to have a huge impact on the wetlands subsidence in Plaquemines. Levees along the Mississippi River removed the natural, renewal sediment flows that are needed to keep the Mississippi River Delta from sinking. Plaquemines parish is the site of several oil refineries and a base for assistance to offshore oilrigs. Oil and gas extraction has also hastened land subsidence protected by the levees in Plaquemines [49].

5. Discussion

Elevation change is a complex process caused by subsidence, as well as changes in sedimentation and human activities. Decreasing elevation does not appear to affect land loss for areas with high elevation or long distances from open water. For coastal area, current elevation strongly determines the impact of subsidence on land loss in the LMRB, especially for the southern parishes adjacent to the Gulf of Mexico. The bubble graph in Figure 5 illustrates the averages of subsidence rates and elevations, together with the population for each parish to explore the relationships of the three elements at the parish scale. The circle size represents the total population within each parish in 2012. For ease of

visualization, the north inland parishes of Washington, West Feliciana, East Feliciana and St. Helena are not shown because of their high mean elevation (40.96–61.78 meters) and relatively low subsidence rates (4.1–6.6 mm/year). Parishes in the south zone are closer to the Gulf of Mexico and have lower elevation and higher subsidence rates. Subsidence-induced elevation change may cause severe land loss and hazard damages in the future, since some of the parishes in the south have large populations such as Orleans and Jefferson.

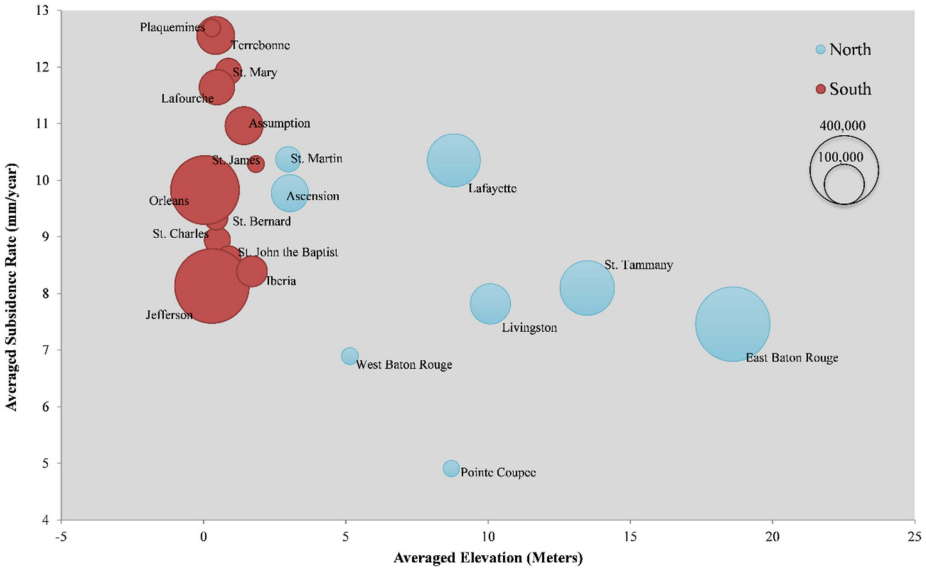

Figure 5. Parish-level average elevation, subsidence rates and population in the LMRB in 2012 (Washington, West Feliciana, East Feliciana and St. Helena parishes are not included).

Using the interpolated rates, we projected the future elevations in 2030 and 2050 assuming that elevation is under the influence of subsidence only, as shown in Figure 6. Areas below sea level are highlighted as red areas and defined as vulnerable regions, which have high potential for land loss. In 2004, only 3.86% of the whole study region, including 0.69% in the north and 7.17% in the south, is below sea level. The most vulnerable regions are located in Orleans parish. If subsidence continues at the current rate, the proportions of vulnerable regions in the north, the south and the whole LMRB will increase to 2.32%, 37.95% and 19.79% in 2030 and to 5.63%, 57.32% and 30.88% in 2050, respectively. In addition to Orleans parish, five more parishes, including Terrebonne, St. Bernard, Plaquemine, Jefferson and Lafourche, will have more than 40% vulnerable regions in their parishes in 2030. By 2050, three more parishes, St. Charles, St. John the Baptist and St. Mary parishes, will join the list of parishes that have more than 40% of the parish area below sea level.

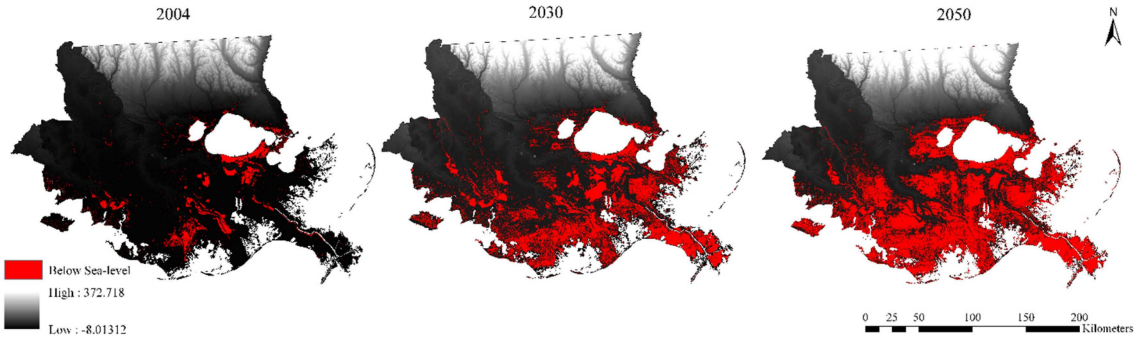

Figure 6. Projected elevation map with areas below sea level.

The most immediate consequence of subsidence-induced elevation change is land loss. Land loss risks will be greater in the regions closest to open water. By 2050, the yearly growth of vulnerable lands will increase from 44.3 km^2/year in 2011 to 240.7 km^2/year in 2050 (Figure 7a). Further, land cover types were overlapped with potential land loss regions. The results indicate that by 2050, Lafourche, Plaquemines and Terrebonne parishes will suffer severe loss of wetlands; Orleans and Jefferson parishes will endure serious loss of developed land; and heavy agricultural land loss will take place in Lafourche Parish (Figure 7b).

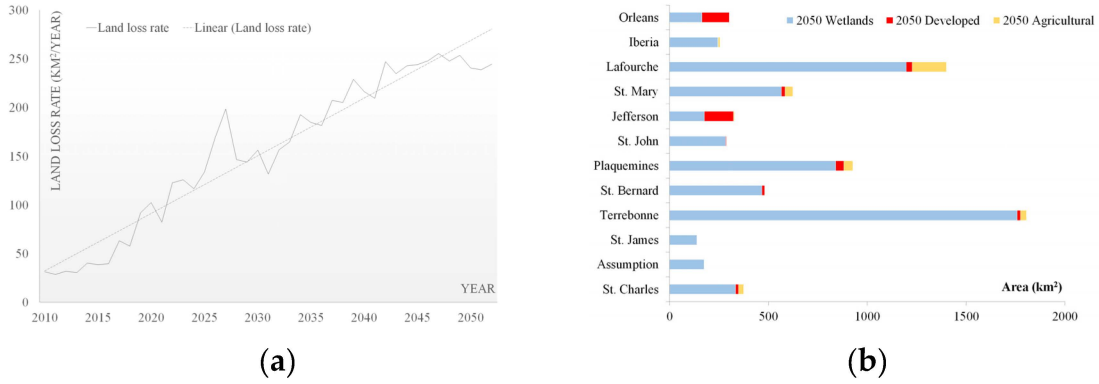

Figure 7. (**a**) Potential land loss rate from 2011 to 2050; (**b**) potential land loss types and areas by parish in the south region.

In reality, subsidence does not necessarily result in land loss. There are multiple, complex natural-human interactions that impact loss and alter local elevation, including sedimentation, hydrocarbon production and construction of levees and canals. Therefore, our estimation may exaggerate the real land loss during the evolution of coastal Louisiana, since the above scenario is based on a single-parameter (subsidence rate) input model. However, land subsidence will still impact population livelihood in profound ways. To protect communities from the consequences of subsidence, such as frequent flooding, governments will have to invest significantly in flood protection levees and pumping stations. Furthermore, Louisiana is a major agricultural state, producing large amounts of rice (ranked third nationally), corn, sugarcane, soybeans and others. Elevation shifting changes the ground's moisture and salinity, which will alter soil availability and decrease yields. Moreover, Louisiana coastal wetlands serve as buffering zones for storms and floods, habitats for aquatic creatures and the base for ecosystem food webs [50]. The abundant aquaculture resources of fishes, oysters, shrimps and crabs contribute to 25% of all seafood in the U.S. and attract numerous tourists from out of state [51]. Even a slight elevation change in wetlands will jeopardize the ecological balance of the wetlands environment, which not only raises the risk of destructive marine forces for human beings, but also threatens local fisheries and tourism.

Despite its contribution towards understanding coastal vertical change, TR50 has been criticized for over-estimating regional subsidence rates [52,53]. Because leveling surveys primarily occurred along transportation corridors, critics contend that the findings in TR50 fail to represent vertical change within the intermediate coastal prairie and wetlands. However, the comparison between EBK, ordinary kriging and the estimates from previous studies (Table 2) reveals comparable findings. The city of New Orleans, which is adjacent to transportation corridors, shows the highest agreements. EBK estimated rates are slightly higher (1–5 mm/year) in most cases of coastal wetlands, except for the Mississippi Deltaic estuary in Plaquemines parish. In general, the subsidence rate layer obtained in this investigation is a reliable reference for modeling scenarios of future environmental changes and identifying regions vulnerable to land loss.

6. Conclusions

This study created a surface representing the general subsidence pattern and evaluated its potential impacts on land loss in the Lower Mississippi River Basin (LMRB). Using the 1178 benchmarks' elevation data for 1922–1995, subsidence rates at 30 m × 30 m were calculated under the consideration of global sea level rise using the ordinary kriging (OK) and empirical Bayesian kriging (EBK) interpolation methods. The results show that the subsidence rates derived by OK and EBK for the entire region ranged from 2.6 to 21.5 and from 1.7 to 29 mm/year, with an average rate of 9 and 9.4 mm/year, respectively. Compared to OK, subsidence rates obtained by EBK have higher agreements with previously-published findings. The subsidence rates increased from north (7.5 ± 5 mm/year) to south (11 ± 10 mm/year). By creating surface contours, four areas of high subsidence rates were observed, including two regions in New Orleans and wetlands in Terrebonne and Plaquemines parishes. The former two could be a result of human activities, such as frequent pumping of water and withdrawal of underground water, whereas the latter could be associated with local soil conditions, levee constructions and heavy hydrocarbon production. By combining the subsidence rates with elevation data in 2004, we projected the elevations in 2030 and 2050 and found that areas below sea level will increase from 3.86% in 2004 to 19.79% in 2030 and 30.88% in 2050. By tabulating the land loss projections with land use and land cover data, we found that heavy wetland loss would occur in Lafourche, Plaquemines and Terrebonne parishes. Orleans and Jefferson will suffer severe loss of developed land, and Lafourche will endure high agricultural land loss.

The significance of this investigation is that it produced a subsidence rate surface for the study region using a rigorous geostatistical interpolation procedure. It then provides scenarios of land subsidence that could threaten the region's sustainability. With sea level rising, the problem could be even more serious. The findings from this study will help decision makers formulate better plans for the region. By identifying the developed areas that have high potential of land loss in the following decades, planners could build more levees to protect this area or avoid the development in those areas. New development could be located further inland while allowing access to the coast for economic activities. Information on potential developed land loss will also be beneficial to residents so that they could plan ahead for protecting their properties and lives, such as lifting their houses or moving to higher ground. In future work, Global Positioning System (GPS)-measured subsidence rate and elevation data will be introduced to validate and calibrate our current estimation to provide a more accurate subsidence rate layer. In addition, frequent hurricanes and flooding in coastal Louisiana will distribute sediment to vulnerable regions and compensate the elevation decrease caused by subsidence. Constructed levees protect low elevation areas (e.g., New Orleans) from both river flooding and land loss. Hence, factors such as sedimentation rates, hydrocarbon production and levee distribution will be considered in modeling elevation change and estimating land loss to project a more realistic future landscape.

Acknowledgments: This research was funded in part by grants from the U.S. National Science Foundation under the Dynamics of Coupled Natural Human Systems (CNH) Program and the Coastal Science, Engineering and Education for Sustainability (Coastal SEES) Program (Award Numbers 1212112 and 1427389). The statements, findings and conclusions are those of the authors and do not necessarily reflect the views of the funding agencies.

Author Contributions: Lei Zou interpolated the subsidence rate layer and prepared the first draft of the manuscript. Joshua Kent provided the subsidence rates dataset and interpreted the results. Nina Lam supervised the data collection and analysis and revised the manuscript. Heng Cai helped with data processing and analysis. All authors read and approved the final manuscript.

Conflicts of Interest: The authors declare no conflict of interest.

References

1. Chan, A.W.; Zoback, M.D. The role of hydrocarbon production on land subsidence and fault reactivation in the Louisiana coastal zone. *J. Coast. Res.* **2007**, *23*, 771–786. [CrossRef]

2. Couvillion, B.R.; Barras, J.A.; Steyer, G.D.; Sleavin, W.; Fischer, M.; Beck, H.; Trahan, N.; Griffin, B.; Heckman, D. Land area change in coastal Louisiana from 1932 to 2010. *U.S. Geological Survey Scientific Investigations Map 3164*; scale 1:265,000. US Geological Survey: Reston, VA, USA, 2011; pp. 1–19.
3. Boesch, D.F.; Josselyn, M.N.; Mehta, A.J.; Morris, J.T.; Nuttle, W.K.; Simenstad, C.A.; Swift, D.J.P. Scientific assessment of coastal wetland loss, restoration and management in Louisiana. *J. Coast. Res.* **1994**, *20*, i-v, 1–103.
4. Morton, R.A.; Bernier, J.C. Recent subsidence-rate reductions in the Mississippi delta and their geological implications. *J. Coast. Res.* **2010**, *263*, 555–561. [CrossRef]
5. Penland, S.; Ramsey, K.E. Relative sea-level rise in Louisiana and the Gulf of Mexico: 1908–1988. *J. Coast. Res.* **1990**, *6*, 323–342.
6. Shinkle, K.D.; Dokka, R.K. *NOAA Technical Report 50: Rates of Vertical Displacement at Benchmarks in the Lower Mississippi Valley and the Northern Gulf Coast*; National Oceanic and Atmospheric Administration, National Geodetic Survey: Sliver Spring, MD, USA, 2004.
7. Meckel, T.A. An attempt to reconcile subsidence rates determined from various techniques in southern Louisiana. *Quat. Sci. Rev.* **2008**, *27*, 1517–1522. [CrossRef]
8. Dixon, T.H.; Amelung, F.; Ferretti, A.; Novali, F.; Rocca, F.; Dokka, R.; Sella, G.; Kim, S.-W.; Wdowinski, S.; Whitman, D. Space geodesy: Subsidence and flooding in New Orleans. *Nature* **2006**, *441*, 587–588. [CrossRef] [PubMed]
9. Yuill, B.; Lavoie, D.; Reed, D.J. Understanding subsidence processes in coastal Louisiana. *J. Coast. Res.* **2009**, *10054*, 23–36. [CrossRef]
10. Xu, Y.J.; Viosca, A. Surface water assessment of three Louisiana watersheds. *Watershed Update* **2005**, *3*, 1–8.
11. Lam, N.S.N.; Arenas, H.; Pace, K.; LeSage, J.; Campanella, R. Predictors of business return in New Orleans after hurricane Katrina. *PLoS ONE* **2012**, *7*. [CrossRef] [PubMed]
12. Grinsted, A.; Moore, J.C.; Jevrejeva, S. Projected Atlantic hurricane surge threat from rising temperatures. *Proc. Natl. Acad. Sci. USA* **2013**, *110*, 5369–5373. [CrossRef] [PubMed]
13. Reed, D.J.; Cahoon, D. Marsh Submergence vs. Marsh Accretion: Interpreting Accretion Deficit Data in Coastal Louisiana. In Proceedings of the 8th Symposium on Coastal and Ocean Management, New Orleans, LA, USA, 19–23 July 1993; pp. 243–257.
14. Britsch, L.D.; Dunbar, J.B. Land loss rates: Louisiana coastal plain. *J. Coast. Res.* **1993**, *9*, 324–338.
15. Roberts, H.H.; Bailey, A.; Kuecher, G.J. Subsidence in the Mississippi river delta—Important influences of valley filling by cyclic deposition, primary consolidation phenomena, and early diagenesis. *Gulf Coast Assoc. Geol. Soc. Trans.* **1994**, *41*, 619–629.
16. Penland, S.; Boyd, R.; Suter, J.R. Transgressive depositional systems of the Mississippi delta plain: A model for barrier shoreline and shelf sand development. *J. Sediment. Res.* **1988**, *58*, 932–949.
17. Penland, S.; Suter, J.R. The geomorphology of the Mississippi River chenier plain. *Mar. Geol.* **1989**, *90*, 231–258. [CrossRef]
18. Ramsey, K.E.; Moslow, T.F. A numerical analysis of subsidence in Louisiana and the Gulf of Mexico. *Gulf Coast Assoc. Geol. Soc. Trans.* **1987**, *39*, 491–500.
19. Kent, J.; Dokka, R. Potential impacts of long-term subsidence on the wetlands and evacuation routes in coastal Louisiana. *GeoJournal* **2013**, *78*, 641–655. [CrossRef]
20. Scardina, A.; Nunn, J.; Pilger, R., Jr. Subsidence and flexure of the lithosphere in the north Louisiana salt basin. *EOS Trans. Am. Geophys. Union* **1981**, *62*, 391.
21. Holzer, T.L.; Bluntzer, R.L. Land subsidence near oil and gas fields, Houston, Texas. *Ground Water* **1984**, *22*, 450–459. [CrossRef]
22. Kooi, H.; de Vries, J.J. Land subsidence and hydrodynamic compaction of sedimentary basins. *Hydrol. Earth Syst. Sci.* **1998**, *2*, 159–171. [CrossRef]
23. Gagliano, S.M.; Kemp, E.B.; Wicker, K.M.; Wiltenmuth, K.S.; Sabate, R.W. Neo-tectonic framework of southeast Louisiana and applications to coastal restoration. *Gulf Coast Assoc. Geol. Soc. Trans.* **2003**, *53*, 262–276.
24. Morton, R.A.; Bernier, J.C.; Barras, J.A.; Ferina, N.F. *Rapid Subsidence and Historical Wetland Loss in the Mississippi Delta Plain: Likely Causes and Future Implications*; 2005–1216; U.S. Geological Survey (USGS): Reston, VA, USA, 2005.

25. Mallman, E.P.; Zoback, M.D. Subsidence in the Louisiana coastal zone due to hydrocarbon production. *J. Coast. Res.* **2007**, *23*, 443–449.
26. Qiang, Y.; Lam, N.N. Modeling land use and land cover changes in a vulnerable coastal region using artificial neural networks and cellular automata. *Environ. Monit. Assess.* **2015**, *187*, 1–16. [CrossRef] [PubMed]
27. Anderson, J.R.; Hardy, E.E.; Roach, J.T.; Witmer, R.E. *A Land Use and Land Cover Classification System for Use with Remote Sensor Data*; Professional Paper 964; US Government Printing Office: Washington, DC, USA, 1976.
28. Oliver, M.A.; Webster, R. Kriging: A method of interpolation for geographical information systems. *Int. J. Geogr. Inf. Syst.* **1990**, *4*, 313–332. [CrossRef]
29. Chang, K.-T. *Introduction to Geographic Information Systems*, 6th ed.; McGraw-Hill Higher Education: Boston, MA, USA, 2006; pp. 324–332.
30. Cressie, N. Spatial prediction and ordinary kriging. *Math Geol.* **1988**, *20*, 405–421. [CrossRef]
31. Lam, N.S.-N. Spatial interpolation methods: A review. *Am. Cartogr.* **1983**, *10*, 129–150. [CrossRef]
32. Pilz, J.; Spöck, G. Why do we need and how should we implement Bayesian Kriging methods. *Stoch. Environ. Res. Risk Assess.* **2008**, *22*, 621–632. [CrossRef]
33. Krivoruchko, K. Empirical bayesian kriging: Implemented in ArcGIS geostatistical analyst. *ArcUser* **2012**, 6–10. Available online: http://www.esri.com/news/arcuser/1012/files/ebk.pdf (accessed on 18 December 2015).
34. Nelson, F.; Hinkel, K.; Shiklomanov, N.; Mueller, G.; Miller, L.; Walker, D. Active-layer thickness in north central Alaska: Systematic sampling, scale, and spatial autocorrelation. *J. Geophys. Res.* **1998**, *103*, 28963–28973. [CrossRef]
35. Peyronnin, N.; Green, M.; Richards, C.P.; Owens, A.; Reed, D.; Chamberlain, J.; Groves, D.G.; Rhinehart, W.K.; Belhadjali, K. Louisiana's 2012 coastal master plan: Overview of a science-based and publicly informed decision-making process. *J. Coast. Res.* **2013**, *67*, 1–15. [CrossRef]
36. Boesch, D.F.; Levin, D.; Nummedal, D.; Bowles, K. *Subsidence in Coastal Louisiana: Causes, Rates, and Effects on Wetlands*; U.S. Fish and Wildlife Service, Division of Biological Services: Washington, DC, USA, 1983.
37. Burkett, V.R.; Zilkoski, D.B.; Hart, D.A. Sea-Level Rise and Subsidence: Implications for Flooding in New Orleans, Louisiana, U.S. In Proceedings of the Geological Survey Subsidence Interest Group Conference: Proceedings of the Technical Meeting, Galveston, TX, USA, 27–29 November 2001; U.S. Geological Survey: Reston, VA, USA, 2003; pp. 63–70.
38. Morton, R.A.; Buster, N.A.; Krohn, M.D. Subsurface controls on historical subsidence rates and associated wetland loss in South-central Louisiana. *Gulf Coast Assoc. Geol. Soc. Trans.* **2002**, *52*, 767–778.
39. Ivins, E.R.; Dokka, R.K.; Blom, R.G. Post-glacial sediment load and subsidence in coastal Louisiana. *Geophys. Res. Lett.* **2007**, *34*. [CrossRef]
40. Lane, R.R.; Day, J.M.; Day, J.N. Wetland surface elevation, vertical accretion, and subsidence at three Louisiana estuaries receiving diverted Mississippi River water. *Wetlands* **2006**, *4*, 1130–1142. [CrossRef]
41. Gagliano, S.M. Effects of Natural Fault Movement on Land Subsidence in Coastal Louisiana. In Proceedings of the 14th Biennial Coastal Zone Conference, New Orleans, LA, USA, 17–21 July 2005.
42. Kuecher, G.J.; Roberts, H.H.; Thompson, M.D.; Matthews, I. Evidence for active growth faulting in the Terrebonne delta plain, south Louisiana: Implications for wetland loss and the vertical migration of petroleum. *Environ. Geosci.* **2001**, *8*, 77–94. [CrossRef]
43. Diegel, F.A.; Karlo, J.F.; Shoup, R.C.; Schuster, D.C. Cenozoic structural evolution and tectono-stratigraphic framework of the northern gulf coast continental margin. *AAPG Memoir* **1996**, *65*, 109–151.
44. Lopez, J.; Penland, S.; Williams, J. Confirmation of active geologic faults in Lake Pontchartrain in southeast Louisiana. *Gulf Coast Assoc. Geol. Soc. Trans.* **1997**, *47*, 299–303.
45. Dokka, R.K. Modern-day tectonic subsidence in coastal louisiana. *Geology* **2006**, *34*, 281–284. [CrossRef]
46. Coastal Wetlands Planning Protection and Restoration Act (CWPPRA). *The Mississippi River Delta Basin*; USGS National Wetlands Research Center: Lafayette, LA, USA, 1999.
47. Coleman, J.; Roberts, H.H. Deltaic coastal wetlands. In *Coastal Lowlands: Geology and Geotechnology*; van der Linden, W.J.M., Cloetingh, S.A.P.L., Kaasschieter, J.P.K., van de Graaff, W.J.E., Vandenberghe, J., van der Gun, J.A.M., Eds.; Springer Netherlands: Dordrecht, The Netherlands, 1989; pp. 1–24.
48. Morton, R.A.; Tiling, G.; Ferina, N.F. *Primary Causes of Wetland Loss at Madison Bay, Terrebonne Parish, Louisiana*; 03-60; USGS, Center for Coastal and Watershed Studies: St. Petersburg, FL, USA, 2003.

49. Plaquemines Parish Comprehensive Master Plan. Coastal Protection and Restoration. *Community Assessment-Technical Addendum, Coastal Protection and Restoration*; Plaquemines Parish Government: Plaquemines Parish, LA, USA, 2015; pp. 1–16.
50. Smith, R.D.; Ammann, A.; Bartoldus, C.; Brinson, M.M. *An Approach for Assessing Wetland Functions Using Hydrogeomorphic Classification, Reference Wetlands, and Functional Indices*; Army Engineer Waterways Experiment Station: Vicksburg, MS, USA, 1995.
51. Coastal Protection & Restoration Authority of Louisiana (CPRA). *Louisiana's Comprehensive Master Plan for a Sustainable Coast*; Coastal Protection and Restoration Authority of Louisiana: Baton Rouge, LA, USA, 2012.
52. González, J.L.; Tornqvist, T.E. Coastal Louisiana in crisis: Subsidence or sea level rise? *Eos Trans. Am. Geophys. Union* **2006**, *87*, 493–498. [CrossRef]
53. Meckel, T.A.; ten Brink, U.S.; Williams, S.J. Current subsidence rates due to compaction of holocene sediments in southern Louisiana. *Geophys. Res. Lett.* **2006**, *33*. [CrossRef]